Hopping conductance and macroscopic quantum tunneling effect in three dimensional $Pb_x(SiO_2)_{1-x}$ nanogranular films

Xiu-Zhi Duan, Zhi-Hao He, Yang Yang, and Zhi-Qing Li*

Tianjin Key Laboratory of Low Dimensional Materials Physics and Preparing Technology, Department of Physics, Tianjin University, Tianjin 300354, China

(Received 16 October 2018; revised manuscript received 22 January 2019; published 18 March 2019)

We have studied the low-temperature electrical transport properties of $Pb_x(SiO_2)_{1-x}$ (x being the Pb volume fraction) nanogranular films with thicknesses of ∼1000 nm and x spanning the dielectric, transitional, and metallic regions. It is found that the percolation threshold x_c lies between 0.57 and 0.60. For films with $x \lesssim 0.50$, the resistivities ρ as functions of temperature T obey a $\rho \propto \exp(\Delta/k_BT)$ relation (Δ being the local superconducting gap and k_B the Boltzmann constant) below the superconducting transition temperature T_c (∼7 K) of Pb granules. The value of the gap obtained via this expression is almost identical to that by single electron tunneling spectra measurement. The magnetoresistance is negative below T_c and its absolute value is far larger than that above T_c at a certain field. These observations indicate that single electron hopping (or tunneling), rather than Cooper pair hopping (or tunneling), governs the transport processes below T_c. The temperature dependence of resistivities shows reentrant behavior for the $0.50 < x < 0.57$ films. This effect is a consequence of the competition between resistance decrease due to the occurrence of superconductivity on isolated Pb grains and the enhancement of excitation resistance due to the opening of the energy gap on the grains. For the $0.60 \lesssim x \lesssim 0.72$ films, the resistivities sharply decrease with decreasing temperature just below T_c, and then show a dissipation effect with further decreasing temperature. Treating the conducting paths composed of Pb particles as nanowires, we have found that the $R(T)$ data below T_c can be well explained by a model that includes both thermally activated phase slips and quantum phase slips.

DOI: 10.1103/PhysRevB.99.094204

I. INTRODUCTION

The transport properties near the superconductor-insulator transition (SIT) in disordered systems continue to attract intense theoretical and experimental interest [1–25]. In this regard, significant attention has been paid to two limiting disordered material systems, the uniform and granular systems. Here the uniform cases are referred to the systems with a potential inhomogeneity only on an atomic scale, while the materials with inhomogeneities that substantially exceed atomic dimensions are called granular systems. For the uniform cases, extensive investigations have been carried out on two dimensional (2D) systems and a wealth of unusual and striking phenomena, including the quantum dissipation in the vortex state [11], the quantum metallic state [21,22], Berezinskii-Kosterlitz-Thouless (BKT) transition [18], and the universal scaling relation for sheet resistance with magnetic field and temperature [11,26], have been revealed. For the granular systems, early studies near the SIT were focused on the origin of critical sheet resistance $R_c = h/(2e)^2$ (where h is the Planck constant and e is the electronic charge) for the onset of superconductivity in 2D films [1–7]. The renewed interest was partially spurred by the theoretical suggestion of disorder-induced spatial inhomogeneity in the superconducting order parameters [27]. It was noted that the high-temperature superconductors are intrinsically disordered, which could lead to self-induced superconducting droplets and render the originally uniform system nonuniform [28,29].

For the granular superconductors, the previous results on the temperature-dependent behaviors of the resistivity below the superconducting transition temperature T_c are quite inconsistent. In discontinuous aluminum [30], Al-Al_2O_3 [31], and Al-Ge [8] films, it has been reported that below T_c the resistivity increases more rapidly with decreasing temperature than that above T_c and the logarithm of the resistivity $\log\rho$ (or $\ln\rho$) increases linearly with $T^{-1/2}$, while in Pb [30], Ga or Al [32], and Bi [32,33] films, it has been found that the resistivity increases exponentially with decreasing temperature below T_c, i.e., $\ln(\rho/\rho_0) \propto 1/T$ with ρ_0 being a constant. In addition, a recent theory [34] predicates that the electron hops via inelastic cotunneling mechanism at $T_1 \lesssim T \lesssim T_c$ in the insulating phase, where $T_1 \approx 0.1\sqrt{E_c\delta}$ is a character temperature, and E_c and δ are the charging energy and the mean energy level spacing in a single grain, respectively. The inelastic cotunneling process would lead to an activation form resistivity. Thus the transport properties of the granular superconductor in the insulating regime need further investigation. On the other hand, the dissipation effect has been observed in the quasi-one-dimensional (1D) superconducting nanowires [35–40] and 2D disordered superconductors [11,18] near the SIT. Thus to check whether the dissipation effect exists in a three dimensional (3D) granular superconductor is interesting and nontrivial.

Considering that Pb is immiscible with SiO_2 and the superconducting transition temperature of granular Pb films is close

*Corresponding author: zhiqingli@tju.edu.cn

to that of the bulk metal [41], we systematically investigate the electrical transport properties of $Pb_x(SiO_2)_{1-x}$ nanogranular films, where x is the volume fraction of Pb. For the insulating films, we found that the temperature dependence of resistivity obeys the activation form the hopping law from $\sim$7 K to T_s (T_s is the temperature below which the resistivity deviates from the activation form law and tends to be saturated; the value of T_s is sample dependent and varies from $\sim$3 to $\sim$4 K for our films), and gradually tends to be saturated with further decreasing temperature below T_s. The dissipation effect is observed in the films with x slightly greater than x_c, where x_c is the percolation threshold above which the films show metallic characteristics in transport properties. We report our interesting observations in the following discussions.

II. EXPERIMENTAL METHOD

Our $Pb_x(SiO_2)_{1-x}$ films were deposited at room temperature by co-sputtering Pb and SiO_2 targets in Ar atmosphere. The details of the deposition procedures were described previously [41]. The $Pb_x(SiO_2)_{1-x}$ films with x ranging from 0.46 to 0.74 were obtained by regulating the sputtering powers in the Pb and SiO_2 targets. The films were simultaneously deposited on the the glass (Fisherfinest premium microscope slides) and polyimide (Kapton) substrates for the transport and composition (polyimide) measurements. For a film with a certain Pb volume fraction x, the powers applied in the two targets are both greater than that used in Ref. [41] for the film with the same x.

The thicknesses of the films ($\sim$1000 nm) were measured using a surface profiler (Dektak, 6M). The Pb volume fraction x in each film was obtained from energy-dispersive x-ray spectroscopy analysis (EDS; EDAX, model Apollo X). The microstructure of the films was characterized by transmission electron microscopy (TEM; Tecnai G2 F20). The TEM cross-section samples were prepared via mechanical cutting, grinding, polishing, and argon ion milling techniques. The films with thickness $\sim$40 nm are deposited on copper grids coated with carbon films and used for top-view TEM measurements. It is found that the cross-sectional TEM image is similar to the top-view image for a certain fixed Pb volume fraction x. The resistivities' variation with temperature, as well as variation with magnetic field, was measured using the standard four-probe method. The temperature and magnetic field environments were provided by a physical property measurement system (PPMS-6000, Quantum Design). For films with large x (small resistivity), both the current source and the voltmeter were provided by the model 6000 PPMS controller, while for the small-x (high-resistivity) films, a Keithley 236 and a Keithley 2182A were used as current source and voltmeter, respectively. The narrow rectangle shape films (2 mm $\times$ 10 mm), defined by mechanical masks, were used for transport measurement. To obtain good contact, the Ti/Au electrodes were deposited on the films.

III. RESULTS AND DISCUSSION

Figure 1 shows the bright-field cross-sectional TEM images of four representative films with $x = 0.47$, 0.50, 0.60, and 0.65. The bright and dark regions in each image are SiO_2 and Pb, respectively. Only the diffraction corresponding to face-centered cubic Pb can be observed in the selected-area electron-diffraction pattern (the inset in Fig. 1), indicating that SiO_2 is amorphous. The mean size of Pb grains, a, obtained by taking into account $\sim$200 grains for each film, increases with increasing x. It is found that mean sizes of Pb grains are less than $\sim$8 nm for the $0.47 \lesssim x \lesssim 0.50$ films, and about $\sim$9 nm for the $0.51 \lesssim x \lesssim 0.60$ films, then vary between $\sim$11 and $\sim$17 nm for the $0.65 \lesssim x \lesssim 0.74$ films. For the film with a certain x, the mean size of Pb granules is not completely identical to that reported in Ref. [41], which could mainly be caused by the differences in sputtering powers.

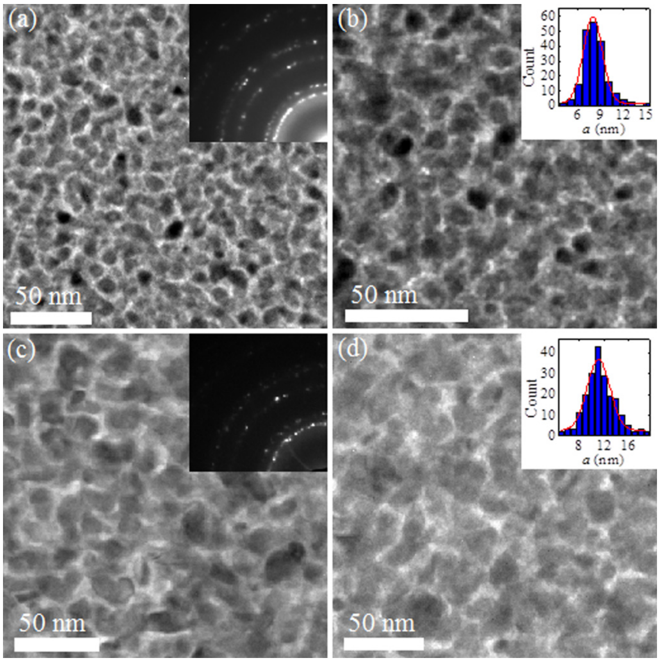

FIG. 1. Bright-field TEM images for $Pb_x(SiO_2)_{1-x}$ films with x values of (a) 0.47, (b) 0.50, (c) 0.60, and (d) 0.65. The insets in (a) and (c) are the selected-area electron-diffraction patterns of corresponding films, and the insets in (b) and (d) show the corresponding grain-size distribution histograms.

Figure 2 shows temperature dependence of normalized resistivity from 300 down to 10 K for some representative films, as indicated. The resistivities of the $x \lesssim 0.57$ films increase with decreasing temperature in this temperature range, while the resistivity decreases with decreasing temperature for the $x \gtrsim 0.60$ films. Thus the percolation threshold x_c for the metal-insulator transition lies between 0.57 and 0.60, which is identical to that reported in Ref. [41]. Next, we discuss the low-temperature electrical transport properties of the films with $x < x_c$ and $x \gtrsim x_c$ in detail.

A. Hopping conductance in the insulating regime

Figure 3(a) shows the resistivity as a function of $T^{-1/2}$ in a single logarithmic scale for three $x < 0.50$ films, as indicated. From $\sim$40 down to $\sim$8 K, the $\log\rho$ (or $\ln\rho$) of each film varies linearly with $T^{-1/2}$, i.e.,

$$\rho = \rho_{01} \exp\left(\frac{T_0}{T}\right)^{1/2}, \tag{1}$$

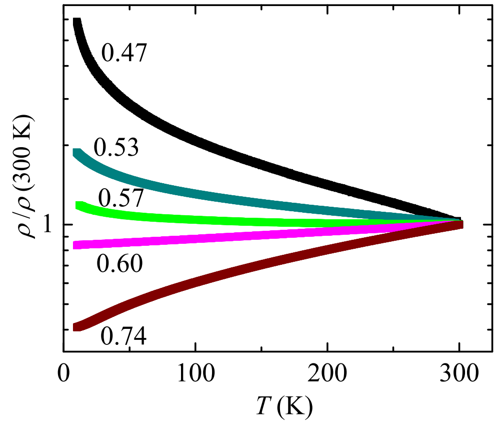

FIG. 2. Normalized resistivity as a function of temperature from 300 down to 10 K for the films with $x \simeq 0.47, 0.53, 0.57, 0.60$, and 0.74.

with ρ_{01} being a constant independent of temperature and T_0 a material-dependent constant. The behavior of resistivity described by Eq. (1) often appears in disordered semiconductors [42–46] and insulating regime of granular metals [47,48]. In disordered semiconductors, the Coulomb interactions between the charge carriers open a Coulomb gap near the Fermi level, which causes the Mott-type variable-range-hopping (VRH) conduction process to cross over to the Efros-Shklovskii-type VRH process when the temperature is sufficiently low [42,43]. Thus the transport process determined by Eq. (1) in disordered semiconductors is called Efros-Shklovskii-type VRH conduction. In granular metals, Sheng and coworkers [47,48] and Wu *et al.* [49] have considered the nonuniformity of the metallic granule size and analyzed the conduction process of thermally activated charge carriers through the percolation path. Then Eq. (1) could be obtained. Recently, several researchers coming from different groups have reconsidered the origin of Eq. (1) in the insulator phase

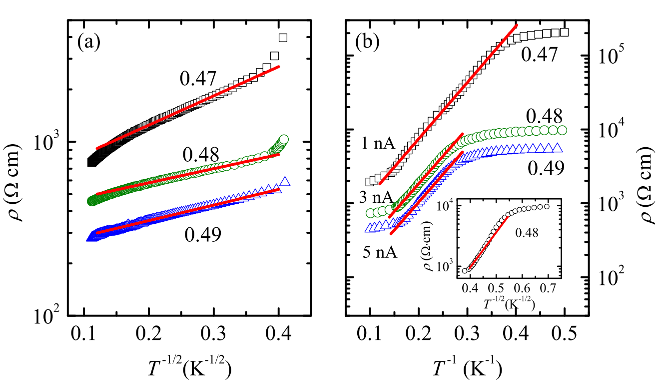

FIG. 3. (a) Logarithm of resistivity as a function of $T^{-1/2}$ from 80 down to 6 K for the $x \simeq 0.47$, 0.48, and 0.49 films. The symbols are the experimental data and the straight solid lines are least-squares fits to Eq. (1). (b) Logarithm of resistivity as a function of the reciprocal of temperature from 10 down to 2 K for the same films in (a). The symbols are the experimental data and the straight solid lines are least-squares fits to Eq. (2). The inset represents the logarithm of resistivity as a function of $T^{-1/2}$ from 8 to 2 K for the $x \simeq 0.48$ film.

of granular metals [50–52]. They have suggested that the "soft gap", being similar to the Coulomb gap, still exists in the granular metals, and the electron conduction can occur through "cotunneling" of electrons between distant metallic granules via a chain of intermediate virtual states.

The solid lines in Fig. 3(a) are least-squares fits to Eq. (1). The value of the adjustable parameter T_0 is listed in Table I. Inspection of Table I indicates that the value of T_0 for the $x \simeq 0.47$ film is much greater than that of other films. In fact, the resistivity of the $x \simeq 0.46$ film is ~50 times as large as that of the $x \simeq 0.47$ film at 300 K and increases with decreasing temperature. Below ~55 K, the resistance of the $x \simeq 0.46$ film exceeds the upper limit (~0.55GΩ) of our measurement unit. Hence $x \simeq 0.47$ is the upper bound of another critical volume fraction below which the $Pb_x(SiO_2)_{1-x}$ films cross into a more insulating region. Similar phenomena (multiple percolation transitions) have been theoretically predicated [53,54] and experimentally observed in Ag-SnO_2 [55], Ag-Al_2O_3 [56], and RuO_2-$CaCu_3Ti_4O_{12}$ [57] granular systems. Here we do not give a detailed discussion on which model is more suitable for our data, and emphasize that the $\rho(T)$ data for the $x \lesssim 0.5$ films obey the widely observed temperature dependence of granular hopping conduction, Eq. (1), from ~40 down to ~8 K.

Figure 3(b) shows the logarithm of the resistivity as a function of the reciprocal of temperature from 10 down to 2 K for the $x < 0.50$ films, as indicated. The values of the current applied to the films are also indicated in Fig. 3(b). Below ~7 K, the resistivity increases more quickly with decreasing temperature than that in $T > T_c$ (where T_c is approximately equal to the superconducting transition temperature of bulk Pb), and the logarithm of the resistivity varies linearly with $1/T$ from ~7 K to T_s (T_s is the temperature below which the linear dependence is not satisfied and the resistivity tends to be saturated; the value of T_s is sample dependent and varies from ~3 to ~4 K for our films). Below T_s, the resistivity gradually approaches saturation with further decreasing temperature. The saturation effect in the low-temperature regime was also observed in quench-condensed Pb granular films and had been ascribed to the negative electroresistance effect below T_c [58]. The inset of Fig. 3(b) shows the resistivity as a function of $T^{-1/2}$ for the $x \simeq 0.48$ film below ~7 K. The $\rho(T)$ data clearly deviates from the solid straight line, indicating that the experimental data cannot be described by Eq. (1) at $T \lesssim T_c$.

In the superconductor-insulator granular system, both Cooper pair hopping and single electron hopping processes could occur below T_c at the insulating regime. For $E_c > \Delta$ (where Δ is the superconducting gap), the transport is mediated by single electron hopping (or tunneling), while the hopping of Cooper pairs dominates the transport process for the opposite case [34,59]. In the former situation, the temperature dependence of the concentration of single electron excitations in superconducting granules obeys $n \propto \exp(-\Delta/k_B T)$ for $T < T_c$. Thus the resistivity variation with temperature can be written as [16]

$$\rho = \rho_{02} \exp\left(\frac{\Delta}{k_B T}\right), \qquad (2)$$

TABLE I. Relevant parameters for some $Pb_x(SiO_2)_{1-x}$ films. Here x is volume fraction of Pb, a is the mean grain diameter, ρ_{01} and T_0 are the parameters in Eq. (1), ρ_{02} and Δ_{01} are the parameters in Eq. (2), Δ_{02} is the deduced zero-temperature superconducting gap by considering the temperature effect of Δ in Eq. (2). E_c is the charging energy and E_J is the Josephson energy between neighbor grains.

x	a (nm)	ρ(300 K) (Ω cm)	ρ(10 K) (Ω cm)	ρ_{01} (10^2 Ω cm)	T_0 (K)	ρ_{02} (Ω cm)	Δ_{01} (meV)	Δ_{02} (meV)	E_c (meV)	E_J (meV)
0.47	7.1	3.29×10^2	1.94×10^3	5.76	14.94	222	1.51	1.16	5.91	1.68×10^{-6}
0.48	7.5	2.94×10^2	7.24×10^2	4.00	3.50	58.0	1.49	0.99	5.37	4.72×10^{-6}
0.49	7.5	2.04×10^2	4.48×10^2	2.34	4.22	32.1	1.50	1.02	5.44	7.58×10^{-6}
0.50	7.9	6.68×10^1	1.37×10^2	0.79	3.00	10.9	1.51	0.95	4.97	2.59×10^{-5}
0.51	8.7	5.44×10^1	9.89×10^1						4.15	3.93×10^{-5}
0.52	9.0	1.49×10^1	3.19×10^1						3.93	1.25×10^{-4}
0.53	9.2	1.11	2.09						3.76	1.95×10^{-3}
0.57	9.2	1.03	1.23						3.76	3.32×10^{-3}
0.60	9.3	1.22×10^{-1}	1.02×10^{-1}							
0.65	11.1	6.57×10^{-2}	5.27×10^{-2}							
0.72	16.0	8.90×10^{-3}	5.30×10^{-3}							
0.73	16.0	5.48×10^{-3}	2.64×10^{-3}							
0.74	16.9	1.68×10^{-3}	6.86×10^{-4}							

where ρ_{02} is a prefactor. For the granular superconductor systems, Efetov once gave an effective Hamiltonian and constructed an analytically solvable model, in which Eq. (2) could be naturally obtained [60]. First, we assume Δ to be a constant and designate it by Δ_{01}. The predications of Eq. (2) are least-squares fitted to the experimental $\rho(T)$ data in the $\ln\rho \propto 1/T$ region and shown by the solid straight lines in Fig. 3(b). The fitted values of the adjustable parameters ρ_{02} and Δ_{01} are listed in Table I. Inspection of Table I indicates that values of Δ_{01} are $\sim$1.50 meV (for all the films), which is almost identical to the zero-temperature superconducting gap Δ_0 of Pb ($\sim$1.37 meV) obtained from single electron tunneling spectra measurements [61]. Thus our experimental results indicate that Eq. (2) is quantitatively applicable in the 3D $Pb_x(SiO_2)_{1-x}$ granular superconductor films in the insulating regime.

Now, we consider the influence of temperature on the width of the superconducting gap. We rewrite Eq. (2) as $\ln\rho = \ln\rho_0 + \Delta_0\delta/k_BT$ with $\delta = \Delta(T)/\Delta_0$. The temperature dependence of $\Delta(T)$ can be obtained from the Bardeen-Cooper-Schrieffer (BCS) theory [62]. The value of Δ_0 is then obtained from the slope of the $\ln\rho$ versus δ/T plot. The values of Δ_0 (denoted as Δ_{02}) for the $x \simeq 0.47$, 0.48, 0.49, and 0.50 films are summarized in Table I. The magnitudes of Δ_{02} are about 15% to 30% less than that obtained by the single electron tunneling method [61]. Thus the relative deviation of Δ_{02} is larger than that by assuming $\Delta \equiv \Delta_0$ in Eq. (2), which in turn indicates that Eq. (2) can be safely used by treating Δ as a constant.

Recently, the hopping transport in granular superconductors in the weak-coupling insulating regime has been theoretically investigated [34]. It has been proposed that the inelastic cotunneling mechanism dominates the single electron hopping process in the temperature region $T_1 \lesssim T \lesssim T_c$, where $T_1 \approx 0.1\sqrt{E_c\delta}$. Due to opening the superconducting gap, the temperature dependence of the resistivity obeys an activation form [34],

$$\rho = \rho_{03}\left(\frac{\bar{E}^2}{4\bar{g}\Delta k_BT}\right)^N \exp\left(\frac{2N\Delta}{k_BT}\right), \tag{3}$$

where $\bar{g}$ and $\bar{E} \sim E_c$ are the typical values of the conductance and Coulomb correlation energy, respectively, ρ_{03} is a constant, and N is the typical tunneling order. The value of charging energy E_c (or $\bar{E}$) can be estimated through $E_c = e^2/(4\pi\epsilon_0\tilde{\kappa}a)$, where a is the mean grain diameter, ϵ_0 is the permittivity of free space, and $\tilde{\kappa} = \epsilon_r[1 + (a/2s)]$ [48] (with ϵ_r being the dielectric constant of the surrounding medium and s the separation between two adjacent grains) is the effective dielectric constant. Taking Δ as the gap value of bulk Pb at $T = 0$, and N, ρ_{03}, and $\bar{g}$ as adjustable parameters, we compare our experimental $\rho(T)$ data with the theoretical predications of Eq. (3). The results indicate that the $\rho(T)$ data can be well described by Eq. (3) from $\sim$7 down to $\sim$3 K for the $x \simeq 0.47$, 0.48, 0.49, 0.50 films. However, the values of the adjustable parameter N are $N \simeq 0.50$ for all the films. Theoretically, the tunneling order N should be $N \gtrsim 2$. Thus the fact that $N \simeq 0.50$ for all films reveals that the inelastic cotunneling process does not occur in the $Pb_x(SiO_2)_{1-x}$ films in the insulating regime. On the other hand, the temperature behavior of $\rho(T)$ in Eq. (3) is mainly determined by the exponential factor; thus $N \simeq 0.50$ implies that the model described by Eq. (2) can be well account for by the hopping transport in the 3D $Pb_x(SiO_2)_{1-x}$ films.

Figure 4(a) shows the resistivity as a function of the reciprocal of temperature under different fields from 10 to 2 K for the $x \simeq 0.48$ film. At a certain temperature, the resistivity decreases with increasing field, which becomes remarkable below $\sim$7 K. Since the magnetic field could lead to suppression of the superconductor ordering parameter and decrease of the Josephson coupling, the negative magnetoresistance clearly indicates that the transport in the $x \lesssim 0.50$ films is governed by the hopping of electrons instead of hopping of Cooper pairs. When the magnetic field is applied, the $\ln(\rho/\rho_{02}) \propto 1/T$ law is still satisfied below $\sim$7 K. The ρ-T curves under 5, 8, and 9 T are also least-squares fitted to Eq. (2) (solid straight lines), and the corresponding values of Δ are 1.13, 0.67, and 0.46 meV, respectively. The field narrows the width of the local superconducting gap; however, local superconductivity has not been completely suppressed; even the magnitude of the field is as large as 9 T.

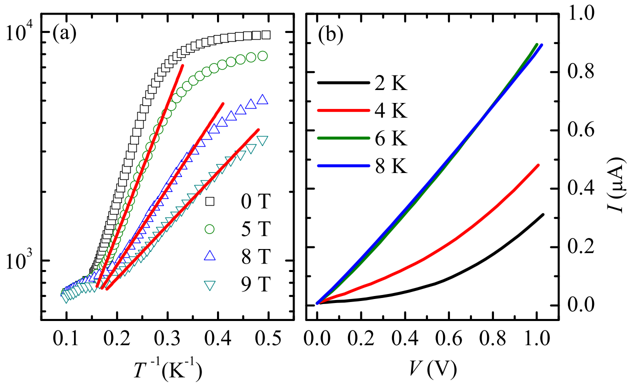

FIG. 4. (a) Logarithm of resistivity as a function of the reciprocal of temperature from 10 down to 2 K under different fields for the $x \simeq 0.48$ film. (b) Current I versus voltage V at different temperatures for the $x \simeq 0.50$ film.

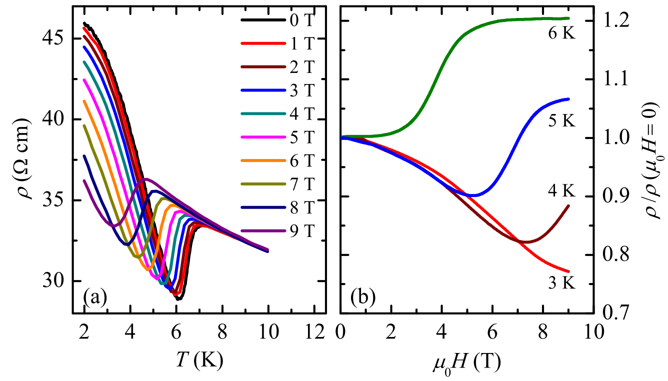

FIG. 5. (a) Resistivity versus temperature under different field for the $x \simeq 0.52$ film. (b) Resistivity versus magnetic field at different temperatures. The μ_0 in the title of the abscissa is the permeability of free space.

In Fig. 4(b), we present the current I as a function of voltage V for the $x \simeq 0.50$ film. Below $\sim$7 K, the current varies nonlinearly with the voltage at the higher voltage region and no hysteresis is observed in the I-V loci. At a certain temperature, the resistance (V/I) decreases with increasing of the applied voltage at the higher voltage region, which indicates a negative electroresistance effect in the film. This confirms that the saturation effect of resistivity at the low-temperature region originates from the negative electroresistance effect of the films [58]. In the ρ-T data measurements, although we take the current as low as possible, as indicated in Fig. 3(b), the saturation effect is still not avoided.

Before ending this subsection, we compare the Josephson energy with the charging energy for the films. The Josephson energy E_J (at $T = 0$) between neighbor grains can be expressed as $E_J = \pi\hbar\Delta_0/(4e^2R_N)$ [63,64], with R_N being the normal-state resistance between two grains. Assuming the system is composed of simple cubic array of metal spheres of diameter a with nearest-neighbor distance $s + a$, one can obtain the relation, $R_N = \rho_N/(s + a)$, where ρ_N is the normal-state resistivity of the system. For the simple cubic model, the separation between two adjacent grains s can be written as $s = a[(\pi/6x)^{1/3} - 1]$ [48] in the dielectric regime. For the $x \lesssim 0.57$ films, the value of the Josephson energy, as well as the charging energy, is listed in Table I. Here the $x \simeq 0.53$ and 0.57 films share the value of s of the $x \simeq 0.52$ film, and ρ_N is taken as the value of resistivity at 10 K for each film. From Table I, one can see that the charging energy is far greater than the Josephson energy for the $x \lesssim 0.57$ films (thus x is also less than x_c). According to the Anderson-Abeles condition [63,65], $E_c \gg E_J$ means the superconducting coupling between the grains is quenched, which is just what we observed in the $x < x_c$ films.

B. Reentrant behavior of the resistivity

Figure 5(a) shows the resistivity as a function of temperature from 10 to 2 K for the $x \simeq 0.52$ film at different field, as indicated. In fact, the variation of resistivity with temperature and magnetic field for the $0.50 < x < 0.57$ films is similar to that of the $x \simeq 0.52$ film. From Fig. 5(a), one can see that the temperature coefficient of resistivity (TCR) $(1/\rho)d\rho/dT$ remains negative above $\sim$7.2 K; then the resistivity sharply decreases with decreasing temperature, reaches its minimum at $T_{\min}$, and then increases again with further decreasing temperature. This reentrant behavior of resistivity is prevalent in the 2D granular superconducting films near the SIT [7] and absent in disordered homogeneous superconducting films [16,32,66]. Kunchur *et al.* observed the reentrant behavior in 3D granular Al films [31]. Combining with the results of Kunchur *et al.*, it can be concluded that the reentrant behavior of resistivity is also prevailing in 3D granular superconductors and occurs in the insulating side of the films with x slightly lower than x_c.

A systematic theoretical description of the reentrant phenomenon is still absent. Fisher once gave an explanation to the reentrant behavior of the resistivity [67]. According to Fisher, the drop in resistivity just below T_c (where T_c is the superconducting transition temperature of the superconductor granules) arises from the shorting out of a portion of the sample by superconducting regions, and quantum tunneling will induce phase slips across the links (barriers), leading to an enhancement of the resistance at sufficiently low temperature. In the framework of this scenario, the magnetoresistance at the low-temperature regime would be positive since the magnetic field results in suppression of the order parameter of the superconductor. To explain the "double reentrance" phenomenon in ultrathin granular films of amorphous bismuth, Parendo *et al.* [66] have proposed that the "reentrant insulator behavior" is the consequence of competition between the drop in resistance due to the occurrence of superconductivity on isolated grain and the enhancement of the resistance due to the opening of the energy gap on the superconducting grains or clusters coupled by quasiparticle tunneling. Beloborodov *et al.* [13] have also proposed a similar explanation, in which the drop in resistivity is attributed to the fluctuation contribution of the Cooper pairs.

Figure 5(b) shows the resistivity as a function of field at different temperatures for the $x \simeq 0.52$ film. At 3 K, the magnetoresistance of the film remains negative up to 9 T, while the resistivity decreases with increasing field, reaches its minimum, and then increases with further increasing of the

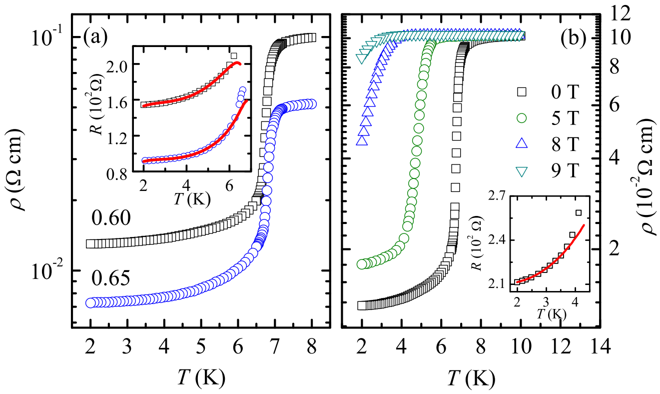

FIG. 6. (a) Resistivity as a function of temperature for $x \simeq 0.60$ and 0.65 films. Inset: Resistance versus temperature below ~6.5 K for the two films. The solid curves are fits to Eq. (4). (b) Resistivity as a function of temperature under different fields for the $x \simeq 0.60$ film. Inset: Resistance versus temperature under 5 T below ~4.5 K for the film. The solid curve is the fit to Eq. (4).

field at relatively higher temperatures (such as 4 K and 5 K). Above ~6 K, the magnetoresistance remains positive over the whole measured field range. The negative low-temperature magnetoresistance indicates that the quantum tunneling induced phase slips is not the dominant mechanism for the reentrance to the insulating phase. According to the scenario of Parendo *et al.* [66] and Beloborodov *et al.* [13], when an intermediate magnetic field is applied, the energy gap would be suppressed, which leads to the reduction of the superconducting transition temperature and an enhancement of the low-temperature excitations. Thus the experimental fact of the gradual reduction in both transition temperature and low-temperature resistivity with increasing magnetic field provides strong support for the pictures of Parendo *et al.* [66] and Beloborodov *et al.* [13]. In Al-Ge granular films, it is found that the high-field ($H > H_c$ with H_c being the intragranular critical field) magnetoresistance is negative for both the insulating film and global superconducting film [8]. Theoretically, Beloborodov *et al.* [10,68] have systematically investigated the high-field negative magnetoresistance phenomena in granular superconductors with large intergrain tunneling amplitude and suggested that superconducting fluctuation, leading to the virtual Cooper pairs and reducing the density of states, is retained at low temperature and $H > H_c$. The fluctuation would be suppressed with further increasing of the magnetic field, which could improve the conductivity and lead to the negative magnetoresistance. According to Fig. 4(a), Fig. 5(a), and Ref. [41], the field with magnitude of 9 T is not high enough to destroy the gap and completely suppress the superconductivity in each Pb grain at low temperature. Thus the mechanism of negative magnetoresistance proposed by Beloborodov *et al.* [10,68] is not observed in our $Pb_x(SiO_2)_{1-x}$ films.

C. Dissipation effect in the metallic regime

Figure 6(a) shows the resistivity as a function of temperature for the $x \simeq 0.60$ and 0.65 films, as indicated. The electrical transport properties of the $0.60 \lesssim x \lesssim 0.72$ films are similar to those of the two representative films. Surprisingly, although the $x \simeq 0.60$ and 0.65 films reveal metallic behavior above T_c, i.e., the TCR is positive, global superconductivity does not appear at any film down to 2 K. For the two films, the resistivities drop sharply below ~7 K and are reduced to ~17% ($x \simeq 0.60$ film) and ~20% ($x \simeq 0.65$ film) of the value of the normal state at ~6 K, respectively. Then the resistivities gradually decrease with further decreasing of temperature. Global superconductivity is present in the $x \gtrsim 0.73$ films. It should be noted here that the low-temperature behaviors of the resistivity of the $Pb_x(SiO_2)_{1-x}$ films with $0.60 \lesssim x \lesssim 0.72$ are not completely identical to those reported in Ref. [41]. For example, the $x \simeq 0.60$ film in Ref. [41] reveals global superconductivity while global superconductivity is not present until x reaches ~0.73 in the present paper. The discrepancies could be caused by two reasons. The first one is the differences in sputtering powers for the films with the same x value, which has been mentioned in Sec. II. For films with a certain Pb volume fraction x, the larger sputtering power in the Pb target used in the present paper would cause the disorder level of Pb granules in the film to be higher than that of the film in Ref. [41]. The higher disorder level may promote the dissipation effect and shift the border of global superconductivity to a higher x value. Another reason is the relative large uncertainty of the EDS (about ±5% in our setup), which undoubtedly renders slight fluctuation of the border for global superconductivity. Next we focus our discussion on the $0.60 \lesssim x \lesssim 0.72$ films.

The dissipation effect in superconductors has been observed in quasi-1D superconducting wires [35–40] and 2D superconducting films [11,18] and has been intensively investigated both in experimental and theoretical sides. The earlier understanding of dissipation in 1D superconductors at $T \lesssim T_c$ is based on the work of Langer and Ambegaokar [69] and McCumber and Halperin [70]. According to their picture, the current-carrier state is only metastable, and dissipation occurs when the system passes over a free-energy barrier ΔF to a lower energy state via thermal activation. This process, called the thermal activation phase slip (TAPS), could result in a resistance with scale $\exp(-\Delta F/k_B T)$. From 1988 to 1991, Giordano investigated the transport properties of small-diameter In and Pb-In wires, and found the TAPS process alone cannot explain the dissipation effect well below T_c [35–37]. He suggested that the phase slippage caused by the quantum-mechanical tunneling of the order parameter through the free-energy barrier plays a dominant role at low temperatures. This mechanism for phase slippage is also called macroscopic quantum tunneling (MQT), since it is analogous to the MQT that occurs in tunneling junctions, superconducting quantum-interference devices, and other systems [71–73].

According to the percolation theory [74], above x_c there is at least one conducting path, in which each metallic particle geometrically connects with the nearest neighbors. Thus each conducting path in the metal-insulator nanogranular systems with x slightly greater than x_c can be reasonably treat as a metallic nanowire. We then analyze the resistance tails below T_c for the $0.60 \lesssim x \lesssim 0.72$ films by considering the combination effect of TAPS and MQT. In the low-current limit, the resistance involving both TAPS and MQT effects can be written as [35–38]

$$R = R_{\mathrm{TAPS}} + R_{\mathrm{MQT}} = c_1 \frac{\pi \hbar^2 \Omega_{\mathrm{TAPS}}}{2e^2 k_B T} e^{-\alpha \Delta F / k_B T} + c_2 \frac{\pi \hbar^2 \Omega_{\mathrm{MQT}}}{2e^2 (\hbar/\tau_{\mathrm{GL}})} e^{-\beta \Delta F \tau_{\mathrm{GL}}/\hbar}, \tag{4}$$

where c_1, c_2, α, and β are possible numerical factors, $\Omega_{\mathrm{TAPS}} = (L/\xi)(\Delta F/k_B T)^{1/2}(1/\tau_{\mathrm{GL}})$ and $\Omega_{\mathrm{MQT}} = (L/\xi)[\Delta F/(\hbar/\tau_{\mathrm{GL}})]^{1/2}(1/\tau_{\mathrm{GL}})$ are the attempt frequencies of thermal activation phase slip and quantum phase slip, respectively, and $\Delta F = (8\sqrt{2}/3)(H_c^2/8\pi)A\xi$ is the magnitude of the free-energy barrier. In these expressions, L is the length of the conducting path, H_c and ξ are the thermodynamic critical field and coherence length of the material, A is the cross-section area of the conducting path, and $\tau_{\mathrm{GL}} = \pi\hbar/8k_B(T_c - T)$ is the characteristic relaxation time in the time-dependent Ginzburg-Landau theory.

The thermodynamic critical field and coherence length of bulk Pb are 0.08 T and 87 nm [75], respectively. Taking the length L and area of the cross section A of each conducting path as $L \simeq 5$ mm and $A \simeq a^2$, respectively, we compare the low-temperature resistance $R(T)$ data of the $x \simeq 0.60$ and 0.65 films with the theoretical predication of Eq. (4). The inset of Fig. 6(a) shows the enlarged image of temperature dependence of resistance from 2 to ~6 K for the $x \simeq 0.60$ and 0.65 films. The solid curves are fits to Eq. (4). Clearly, the experimental $R(T)$ data from 2 to ~6 K can be well described by Eq. (4). The values of the adjustable parameters are $c_1 \simeq 5.4 \times 10^{-6}$, $c_2 \simeq 5.5 \times 10^{-5}$, $\alpha \simeq 6976$, and $\beta \simeq 1944$ for the $x \simeq 0.60$ film and $c_1 \simeq 3.3 \times 10^{-6}$, $c_2 \simeq 2.5 \times 10^{-5}$, $\alpha \simeq 5124$, and $\beta \simeq 648$ for the $x \simeq 0.65$ film. The parameters c_1 and c_2 are both far less than unity, while α and β are much greater than unity. These deviations should not be taken too seriously since both the theories of TAPS and MQT are extremely qualitative [36]. On the other hand, there is more than one conducting path in the $x \gtrsim x_c$ films. Hence all the conducting paths connected in parallel and resistance of the film is about $R_{\mathrm{sig}}/\mathfrak{n}$, where R_{sig} is the resistance of a single conducting path and $\mathfrak{n}$ is the number of conducting paths between the two voltage electrodes. Thus the value of c_1 (c_2) should be $1/\mathfrak{n}$ of that for a single conducting path. In addition, the values of the L and A are also quite qualitative, which seriously affects the magnitudes of the numerical factors c_1, c_2, α, and β.

Figure 6(b) shows the temperature dependence of the resistivity for the $x = 0.60$ film at different fields. Inspection of Fig. 6(b) indicates that the transition temperature decreases with increasing magnetic field and the magnetoresistance is positive below ~7 K [76]. Even when a field with magnitude of 5 T is applied, the variation trend of the $\rho(T)$ curve is retained; i.e., the resistance tail also exists at low temperature. In addition, the $R(T)$ curve at 5 T can be also described by Eq. (4) [solid curve in the inset of Fig. 6(b)] below ~4 K, which indicates that both the TAPS and MQT processes are also the main mechanisms of the dissipation effect. The values of the adjustable parameters are $c_1 \simeq 1.6 \times 10^{-6}$, $c_2 \simeq 8.3 \times 10^{-5}$, $\alpha \simeq 3629$, and $\beta \simeq 887$. We note in passing that the dissipation effect in our films is not caused by the granular effect of the system. The positive TCR from 300 down to ~10 K indicates that the nearest-neighbor Pb granules in the conducting path have geometrically connected and there is no insulator barrier between them.

IV. CONCLUSION

We have investigated the electrical transport properties of $Pb_x(SiO_2)_{1-x}$ nanogranular films with $0.46 \lesssim x \lesssim 0.74$. The percolation threshold of this system lies between 0.57 and 0.60. For the $0.47 \lesssim x \lesssim 0.50$ films, the temperature dependence of resistivities obeys a $\rho = \rho_{02}\exp(\Delta/k_B T)$ law from ~7 K to T_s, and the experimental values of Δ are comparable to that obtained in single electron tunneling spectra measurement. Below T_c the magnetoresistance is negative and its absolute value is much larger than that above T_c, which indicates the single electron hopping or tunneling dominates the transport process below T_c. For the $0.50 < x < 0.57$ films, the temperature dependence of resistivities reveals reentrant behavior below T_c. This effect is the consequence of competition between the drop in resistance due to the occurrence of superconductivity on isolated Pb grains and the enhancement of excitation resistance due to the opening of the energy gap on the Pb grains. Although the TCRs of the $0.60 \lesssim x \lesssim 0.72$ films are all positive from 300 down to 10 K, global superconductivity is not present in these films. The resistivities of these films decrease sharply with decreasing temperature at temperature slightly below T_c, and then decrease slowly with further decreasing temperature. We treat the conducting paths as Pb nanowires and have found that the $R(T)$ data below T_c can be well described by the model that includes both thermally activated phase slips and quantum phase slips.

ACKNOWLEDGMENT

This work is supported by the National Natural Science Foundation of China through Grant No. 11774253.

[1] B. G. Orr, H. M. Jaeger, and A. M. Goldman, Phys. Rev. Lett. **53**, 2046 (1984).
[2] B. G. Orr, H. M. Jaeger, and A. M. Goldman, Phys. Rev. B **32**, 7586 (1985).
[3] B. G. Orr, H. M. Jaeger, A. M. Goldman, and C. G. Kuper, Phys. Rev. Lett. **56**, 378 (1986).
[4] H. M. Jaeger, D. B. Haviland, A. M. Goldman, and B. G. Orr, Phys. Rev. B **34**, 4920 (1986).
[5] S. Chakravarty, G. L. Ingold, S. Kivelson, and A. Luther, Phys. Rev. Lett. **56**, 2303 (1986).
[6] S. Chakravarty, S. Kivelson, G. T. Zimanyi, and B. I. Halperin, Phys. Rev. B **35**, 7256 (1987).
[7] H. M. Jaeger, D. B. Haviland, B. G. Orr, and A. M. Goldman, Phys. Rev. B **40**, 182 (1989).
[8] A. Gerber, A. Milner, G. Deutscher, M. Karpovsky, and A. Gladkikh, Phys. Rev. Lett. **78**, 4277 (1997).

[9] A. M. Goldman and N. Marković, Phys. Today **51** (11), 39 (1998).
[10] I. S. Beloborodov and K. B. Efetov, Phys. Rev. Lett. **82**, 3332 (1999).
[11] N. Mason and A. Kapitulnik, Phys. Rev. Lett. **82**, 5341 (1999).
[12] Y. Dubi, Y. Meir, and Y. Avishai, Nature (London) **449**, 876 (2007).
[13] I. S. Beloborodov, A. V. Lopatin, V. M. Vinokur, and K. B. Efetov, Rev. Mod. Phys. **79**, 469 (2007).
[14] T. I. Baturina, C. Strunk, M. R. Baklanov, and A. Satta, Phys. Rev. Lett. **98**, 127003 (2007).
[15] B. Sacépé, C. Chapelier, T. I. Baturina, V. M. Vinokur, M. R. Baklanov, and M. Sanquer, Phys. Rev. Lett. **101**, 157006 (2008).
[16] V. F. Gantmakher and V. T. Dolgopolov, Phys. Usp. **53**, 1 (2010).
[17] K. Bouadim, Y. L. Loh, M. Randeria, and N. Trivedi, Nat. Phys. **7**, 884 (2011).
[18] Y.-H. Lin, J. Nelson, and A. M. Goldman, Phys. Rev. Lett. **109**, 017002 (2012).
[19] M. Ovadia, D. Kalok, B. Sacépé, and D. Shahar, Nat. Phys. **9**, 415 (2013).
[20] I. S. Burmistrov, I. V. Gornyi, and A. D. Mirlin, Phys. Rev. B **92**, 014506 (2015).
[21] Y. Saito, Y. Kasahara, J. Ye, Y. Iwasa, and T. Nojima, Science **350**, 409 (2015).
[22] A. W. Tsen, B. Hunt, Y. D. Kim, Z. J. Yuan, S. Jia, R. J. Cava, J. Hone, P. Kim, C. R. Dean, and A. N. Pasupathy, Nat. Phys. **12**, 208 (2016).
[23] M. Mulligan and S. Raghu, Phys. Rev. B **93**, 205116 (2016).
[24] M. V. Feigel'man and L. B. Ioffe, Phys. Rev. Lett. **120**, 037004 (2018).
[25] Y. J. Fan, C. Ma, T. Y. Wang, C. Zhang, Q. L. Chen, X. Liu, Z. Q. Wang, Q. Li, Y. W. Yin, and X. G. Li, Phys. Rev. B **98**, 064501 (2018).
[26] A. Yazdani and A. Kapitulnik, Phys. Rev. Lett. **74**, 3037 (1995).
[27] M. A. Skvortsov and M. V. Feigel'man, Phys. Rev. Lett. **95**, 057002 (2005).
[28] Y. Imry, M. Strongin, and C. C. Homes, Physica C **468**, 288 (2008).
[29] S. H. Pan, J. P. O'Neal, R. L. Badzey, C. Chamon, H. Ding, J. R. Engelbrecht, Z. Wang, H. Eisaki, S. Uchida, A. K. Gupta, K. W. Ng, E. W. Hudson, K. M. Lang, and J. C. Davis, Nature (London) **413**, 282 (2001).
[30] R. C. Dynes, J. P. Garno, and J. M. Rowell, Phys. Rev. Lett. **40**, 479 (1978).
[31] M. Kunchur, Y. Z. Zhang, P. Lindenfeld, W. L. McLean, and J. S. Brooks, Phys. Rev. B **36**, 4062 (1987).
[32] Y. H. Lin and A. M. Goldman, Phys. Rev. B **82**, 214511 (2010).
[33] M. D. Stewart Jr., A. Yin, J. M. Xu, and J. M. Valles Jr., Science **318**, 1273 (2007).
[34] A. V. Lopatin and V. M. Vinokur, Phys. Rev. B **75**, 092201 (2007).
[35] N. Giordano, Phys. Rev. Lett. **61**, 2137 (1988).
[36] N. Giordano, Phys. Rev. B **41**, 6350 (1990).
[37] N. Giordano, Phys. Rev. B **43**, 160 (1991).
[38] M. Tian, J. Wang, J. S. Kurtz, Y. Liu, M. H. W. Chan, T. S. Mayer, and T. E. Mallouk, Phys. Rev. B **71**, 104521 (2005).
[39] W. Zhao, X. Liu, and M. H. W. Chan, Nano Lett. **16**, 1173 (2016).
[40] J. Kim, B. K. Kim, H. S. Kim, A. Hwang, B. Kim, and Y. J. Doh, Nano Lett. **17**, 6997 (2017).
[41] Y. J. Xi, K. H. Gao, Z. W. Wang, and Z. Q. Li, Phys. Status Solidi RRL **11**, 1700070 (2017).
[42] A. L. Efros and B. I. Shklovskii, J. Phys. C **8**, L49 (1975).
[43] A. L. Efros, J. Phys. C **9**, 2021 (1976).
[44] Y. Zhang, P. Dai, M. Levy, and M. P. Sarachik, Phys. Rev. Lett. **64**, 2687 (1990).
[45] Y. L. Huang, S. P. Chiu, Z. X. Zhu, Z. Q. Li, and J. J. Lin, J. Appl. Phys. **107**, 063715 (2010).
[46] Y. C. Ji, H. X. Zhang, X. H. Zhang, and Z. Q. Li, Phys. Status Solidi B **250**, 2145 (2013).
[47] P. Sheng, B. Abeles, and Y. Arie, Phys. Rev. Lett. **31**, 44 (1973).
[48] B. Abeles, P. Sheng, M. D. Coutts, and Y. Arie, Adv. Phys. **24**, 407 (1975).
[49] T. C. Wu, J. J. Lin, and P. Sheng, Front. Phys. **13**, 137205 (2018).
[50] J. Zhang and B. I. Shklovskii, Phys. Rev. B **70**, 115317 (2004).
[51] T. B. Tran, I. S. Beloborodov, X. M. Lin, T. P. Bigioni, V. M. Vinokur, and H. M. Jaeger, Phys. Rev. Lett. **95**, 076806 (2005).
[52] M. V. Feigel'man and A. S. Ioselevich, Pis'mav Zh. Eksp. Teor. Fiz. **81**, 341 (2005) [JETP Lett. **81**, 277 (2005)].
[53] I. Balberg, J. Phys. D: Appl. Phys. **42**, 064003 (2009).
[54] G. Ambrosetti, I. Balberg, and C. Grimaldi, Phys. Rev. B **82**, 134201 (2010).
[55] Y. F. Wei and Z. Q. Li, Appl. Phys. Lett. **102**, 131911 (2013).
[56] I. Balberg, D. Azulay, J. Jedrzejewski, and E. Savir, Appl. Phys. Lett. **104**, 253109 (2014).
[57] R. Mukherjee, Z. F. Huang, and B. Nadgorny, Appl. Phys. Lett. **105**, 173104 (2014).
[58] R. P. Barber, Jr., S. Y. Hsu, J. M. Valles, Jr., R. C. Dynes, and R. E. Glover, III, Phys. Rev. B **73**, 134516 (2006).
[59] T. Chen, B. Skinner, and B. I. Shklovskii, Phys. Rev. B **86**, 045135 (2012).
[60] K. B. Efetov, Zh. Eksp. Teor. Fiz. **78**, 2017 (1980) [Sov. Phys. JETP **51**, 1015 (1980)].
[61] W. L. McMillan and J. M. Rowell, Phys. Rev. Lett. **14**, 108 (1965).
[62] J. Bardeen, L. N. Cooper, and J. R. Schrieffer, Phys. Rev. **108**, 1175 (1957).
[63] B. Abeles, Phys. Rev. B **15**, 2828 (1977).
[64] G. Deutscher, O. Entin-Wohlman, S. Fishman, and Y. Shapira, Phys. Rev. B **21**, 5041 (1980).
[65] P. W. Anderson, in *Lectures on the Many-Body Problem*, edited by E. R. Caianiello (Academic, New York, 1964), Vol. 2, p. 127.
[66] K. A. Parendo, K. H. S. B. Tan, and A. M. Goldman, Phys. Rev. B **76**, 100508(R) (2007).
[67] M. P. A. Fisher, Phys. Rev. Lett. **57**, 885 (1986).
[68] I. S. Beloborodov, K. B. Efetov, and A. I. Larkin, Phys. Rev. B **61**, 9145 (2000).
[69] J. S. Langer and V. Ambegaokar, Phys. Rev. **164**, 498 (1967).

[70] D. E. McCumber and B. I. Halperin, Phys. Rev. B **1**, 1054 (1970).
[71] R. F. Voss and R. A. Webb, Phys. Rev. Lett. **47**, 265 (1981).
[72] A. O. Caldeira and A. J. Leggett, Phys. Rev. Lett. **46**, 211 (1981).
[73] V. Ambegaokar, U. Eckern, and G. Schön, Phys. Rev. Lett. **48**, 1745 (1982).
[74] R. Zallen, *The Physics of Amorphous Solids* (Wiley, New York, 1983).
[75] W. H. Li, C. C. Yang, F. C. Tsao, and K. C. Lee, Phys. Rev. B **68**, 184507 (2003).
[76] Although global superconductivity is not present in this film, we also designate a transition temperature at which the resistivity has dropped to $\rho_N/2$ with ρ_N being the normal-state resistivity at 10 K.